Focussed on: Computational Mechanics and Mechanics of Materials in Italy

An ideal model for stress-induced martensitic transformations in shape-memory alloys

Michele Marino
Department of Civil Engineering and Computer Science Engineering (DICII), Università degli Studi di Roma Tor Vergata, via del Politecnico 1, 00133 Roma – Italy
m.marino@ing.uniroma2.it

ABSTRACT. In this paper, a novel model for stress-induced martensitic transformations in shape-memory alloys is proposed. Accordingly, the constitutive pseudo-elastic behavior of these materials is described. The model accounts for the possible co-existence of austenitic/martensitic phases and for asymmetric response in tension and compression (both for transformation and stiffness properties).
The model is developed under the assumption of ideal behavior during martensitic transformation, and the predicted response is governed by few parameters, standard in the context of shape-memory alloys' constitutive models, that can be straightforwardly identified from experimental data. Moreover, proposed modeling framework opens to the investigation on the effects of non-linear transformation lines in phase diagrams and of temperature-dependent transformation strains.

KEYWORDS. Shape-memory alloys; Pseudo-elastic behaviour; Constitutive modelling; Stress-induced martensitic transformation.

INTRODUCTION

Shape-memory alloys (SMAs) are special materials endowed of fascinating properties thanks to possible rearrangements of their thermoelastic lattice microstructure, generally referred to as phase transformations. In fact, objects made of those materials, when significantly deformed, regain their original geometric configuration during heating (one-way shape-memory effect) or, at higher temperature, in the unloading phase (pseudo-elasticity).
The intriguing SMA thermomechanical properties allow to design smart structures, opening to innovative applications in many engineering fields. Proposed designs based on such materials range from aeronautic/mechanical applications (e.g., adaptive smart wings and actuators) and telecommunication devices (e.g., deployment and control mechanisms of satellites and antennas), to biomedical (e.g., self-expanding stents, orthodontic wires, and prostheses) and civil applications (e.g., devices for passive, active and semi-active controls of civil structures) [1, 2].
As proved by the recent wide literature in the field [1, 3-5], there is a great need of constitutive models able to reproduce SMAs behavior, including a refined description of phase transformation mechanisms. In order to be effectively employed in practical applications, models should be characterized by parameters whose values have to be easily identified from well-established experimental procedures. Moreover, since there exists a number of different materials with shape-memory and pseudoelastic properties, models should be as flexible as possible in order to be adapted to the wide range of very different thermomechanical features shown through experiments. Finally, models should be formulated within a consistent theoretical framework that, in the respect of thermodynamics laws, might be implemented in feasible numerical algorithms for computational analyses.

In this paper, a novel constitutive model for SMAs is proposed for describing their pseudo-elasticity properties. Accordingly, stress-induced transformations (SITs) are modeled by addressing isothermal uniaxial tests and by considering direct transformations from a non-oriented lattice arrangement (namely, multi-variant martensite Mm or austenite A) to an oriented one (that is, single-variant martensite in its traction and compression variants, Ms+ and Ms-), and viceversa reverse transformations Ms+/Ms- $\rightarrow$ Mm/A,[1].

As a notation rule, quantities referred to Ms+ are indicated by the superscript $+$, and to Ms- by the superscript $-$, while to direct and reverse transformations by subscripts d (or D) and r (or R). Denoting with T_{mf} and T_{af} the zero-stress martensite-finish and austenite-finish characteristic temperatures (namely, Mm is stable at $T < T_{mf}$ and A is stable at $T > T_{af}$), the typical SMA non-linear behavior at high temperature, $T > T_{af}$, and at low-temperature, $T < T_{mf}$, is addressed. Moreover, an intermediate-temperature range, $T_{mf} < T < T_{af}$, is also considered by admitting the co-existence of Mm and A at low stress.

Present model opens to consider the well-established temperature dependence of transformation strains $\varepsilon_{D/R}^{+/-}$ (namely, the strain accumulated during SITs), [6]. Moreover, it is based on a very general phase diagrams with highly non-linear direct/reverse transformation lines $\sigma_{d/r}^{+/-}(T)$ and without the need of fixing a specific form for the interpolation functions describing the stress-temperature dependence (see Fig. 1). In the lack of detailed experimental data, the only assumption on the phase diagram is that there exists a unique temperature value T_{ro}, such that $T_{mf} < T_{ro} < T_{af}$, at which reverse transformations (both from Ms+ and Ms-) occur at zero stress (that is, the temperature corresponding to $\sigma_r^+ = \sigma_r^- = 0$).

The motivations underlying this work, as well as the novelty of the proposed approach with respect to existing modeling approaches, are elucidated in the following.

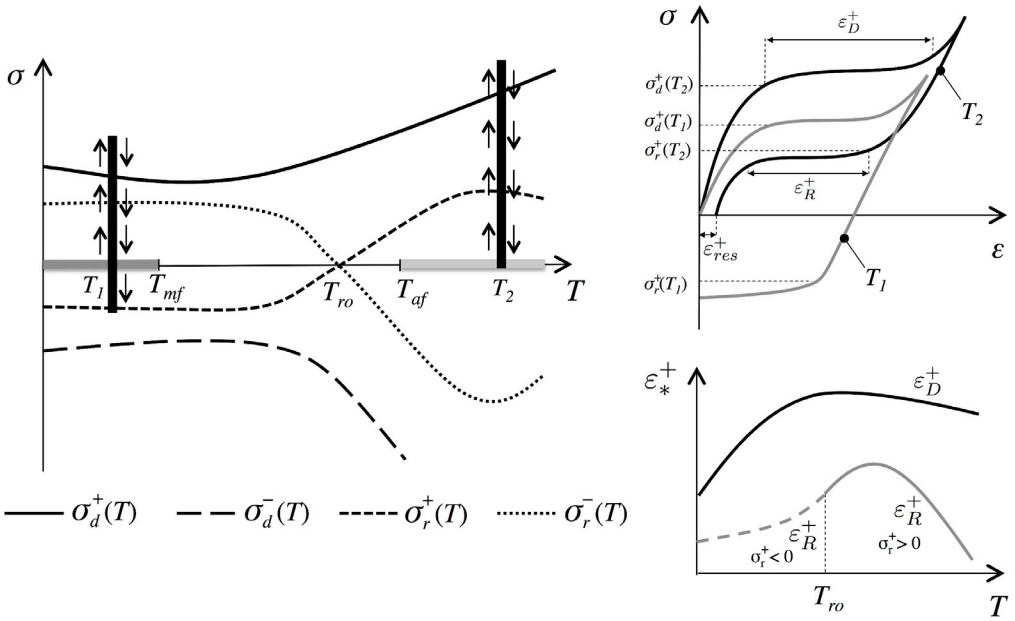

Figure 1: Left: typical phase diagram in σ-T plane for SMAs. The figure shows the direct SIT lines to Ms+ (σ_d^+) and to Ms- (σ_d^-), as well as the reverse ones from Ms+ (σ_r^+) and from Ms- (σ_r^-). Moreover, two loading-unloading paths for uniaxial isothermal traction tests are shown at $T = T_1 < T_{mf}$ and $T = T_2 > T_{af}$. Top right: SMA typical σ-ε constitutive relationship at $T = T_1$ and $T = T_2$. Bottom right: SMA typical relationships between direct (ε_D^+) and reverse (ε_R^+) transformation strains and T.

State-of-the-art and proposed improvements

Existing constitutive relationships for SMAs can be categorized as either micro, micro-macro or macro models [7]. In this paper, phenomenological macro-models are addressed because these are the most effective for engineering applications, being able to describe SMA global structural behavior without an explicit modeling of micro-scale behavior. Parameters of

phenomenological models are usually identified by classical experimental tests and the governing equations are mostly suitable for being implemented into computer programs for structural analyses.
A thorough review of the available phenomenological models in specialized literature can be found in [1]. The sequence of thermodynamic states occurring in SMAs is usually described by introducing additional variables (such as martensite and austenite volume fractions), within the framework of thermodynamics with internal state variables [8]. Current SMA constitutive models have reached a high level of sophistication accounting for multiple and simultaneous thermomechanical mechanisms [3-5, 9-13]. Nevertheless, a common limitation is that most existing models generally assume that phase diagrams governing phase transformations are characterized by piecewise-linear transformation lines, despite of high non-linearities highlighted from experiments [6]. A model overcoming this drawback has been recently addressed by Lagoudas and co-workers [14]. Moreover, different direct and reverse transformation strains (associated with different transformation kinetics), as well as their dependence on temperature, are generally neglected. Furthermore, the implementation of the most effective models is heavy due to:

- the costly calibrations of a high number of model parameters, in some case without a clear physical meaning;
- the need of introducing iterative schemes for satisfying inequality constraints by means of implicit multi-step redictor-corrector schemes or by introducing equivalent non-linear systems in a large number of unknowns.

The last drawback is due to the need of fulfilling the second law of thermodynamics by solving a constrained optimization problem with inequality constraints that derives from the Clausius-Duhem inequality or, equivalently, from Kuhn-Tucker conditions, [4].
On the other hand, as shown by J.J. Moreau [15], the second law of thermodynamics may be *a-priori* satisfied within the energy statement of the problem if the constitutive laws for the dissipative part of the static quantities involved in equilibrium equations are defined through the introduction of a pseudo-potential of dissipation. In this case, no iterative numerical schemes are needed for satisfying energy inequality constraints. Following this thermodynamical framework, Frémond developed a phenomenological SMA model based on internal constraints enforced by means of convex analysis arguments [16]. The rationale is standard, successful in modeling many structural mechanical problems involving phase change [17], and characterized by:

- a proper choice of state variables;
- the formulation of equilibrium equations from the Principle of Virtual Work; if internal variables describing different material phases are introduced as state quantities, equilibrium equations will directly give transformation-evolution laws;
- the introduction of constitutive laws by splitting static quantities (dual to state variables) in terms of their non-dissipative and dissipative term; the former is obtained by the differentiation of the free-energy with respect to state quantities, while the latter by differentiating the pseudo-potential of dissipation with respect to state quantities evolution;
- the enforcement of physical restrictions on state quantities and on their evolution through sub-differentiable indicator functions (valued zero or $+\infty$) added to both the free-energy and the pseudo-potential of dissipation; accordingly, the evolutions of thermomechanical quantities are obtained by projection on convex hulls defining admissible states.

Even if qualitative results of Frémond's model are good, it does not capture all SMA features: no multi-variant martensite volume fraction is considered, the strain-width of the stress-strain loop is proportional to its stress-size, unrealistic softening behavior for strain-driven case arise during direct martensitic transformation in uniaxial isothermal response, austenite and martensite phases have the same material parameters. A further drawback of Frémond's model is that the total transformation strain, which is the quantity characterized during experiments, is not a model parameter and it non-linearly depends on a phase-change viscosity parameter, being of tough determination from experimental data.
Frémond's rationale inspired Baêta-Neves and co-authors, [18, 19], whose model introduces some improvements but it is still characterized by softening behavior if not treated with an augmented Lagrangian method for convexification of system's energy [20]. Accordingly, in order to allow engineers to design shape-memory structures by means of the consistent thermodynamical Moreau's framework in which Frémond's model is formulated, improvements are still necessary.
The constitutive model for the pseudo-elastic behavior of SMAs proposed in the present work is developed in the lines of the Frémond's rationale [16, 17]. Obtained results highlight main model features:

1. different kinetics between direct and reverse phase transformations;
2. asymmetric response of transformation mechanisms in tension and compression;
3. admissibility of the co-existence of austenite, multi-variant and oriented martensites;
4. straightforward material parameter identification;

5. different elastic moduli in tension and compression.

The model is herein developed within a one-dimensional framework by assuming an ideal transformation behavior characterized by no-hardening effects.

Thanks to the employed generalized energetic framework, the second law of thermodynamics is fulfilled without the need of implicit algorithms. Accordingly, thanks to the explicit framework in which present model can be implemented, the model allows to straightforwardly include unconventional SMA features such as

- non-linear transformation lines in a very flexible phase diagram;
- dependence of transformation strains on temperature.

Following the recent works by Lagoudas and co-workers, [14], the possibility to address the non-linear dependence of transformation strains and stresses on temperature is a novelty with respect to many well-established available models.

MODEL

Consider a one-dimensional (1D) material element of infinitesimal length acted by a self-equilibrated Cauchy stress σ at constant temperature T.

The model is based on an incremental approach in the time variable τ. Accordingly, the actual value (at time $\tau = t$) of the strain measure ε is obtained from the superimposition of a reference value $\overline{\varepsilon}$ (at time $\tau = \overline{t}$) with an infinitesimal perturbation $d\varepsilon$ (associated with the time increment dt, where $t = \overline{t} + dt$), resulting $\varepsilon = \overline{\varepsilon} + d\varepsilon$. In order to account for different deformation mechanisms in SMAs and in agreement with available modeling approaches [5, 12, 21], the mapping from the reference to the actual state is regarded as the superimposition of different thermomechanical mechanisms allowing to identify several deformation variables. Accordingly, the infinitesimal strain is split in

$$d\varepsilon = d\varepsilon_e + d\varepsilon_i \tag{1}$$

where subscripts e and i relate the infinitesimal strain with elastic and inelastic mechanisms, respectively. Denoting the time derivative (in the sense of left-derivative with respect to the actual time t in agreement with the causality principle) with the dot superscript, let $\varepsilon_k = \overline{\varepsilon}_k + d\varepsilon_k = \overline{\varepsilon}_k + \dot{\varepsilon}_k dt$ (with $k = \{e,i\}$) be introduced. Within a displacement-based approach, the material element is said to undergo loading conditions if $d\varepsilon \cdot \varepsilon > 0$, and unloading conditions if $d\varepsilon \cdot \varepsilon < 0$.

For describing the alloy composition, quantities β_j (with $j \in \{1,2,3,4\}$) represent respectively the volume fractions of austenite (A), single-variant martensites (Ms+ and Ms-), and multi-variant martensite (Mm).

The initial thermodynamical state (at $\tau = 0$ and denoted by superscript *in*) is assumed to be physically admissible, that is:

1. austenite is not present at low temperatures $\Rightarrow$ if $T < T_{mf}$, then $\beta_1^{in} = 0$;
2. multi-variant martensite is not present at high temperatures $\Rightarrow$ if $T > T_{af}$, then $\beta_4^{in} = 0$;
3. the alloy is aligned either according to the Ms+ or to Ms- configuration $\Rightarrow$ $\beta_2^{in} \cdot \beta_3^{in} = 0$.

Phase volume fractions are not independent, since they satisfy some physical properties due to their definitions or to the mechanical properties assumed in the present work. Accordingly, quantities β_j have to respect the following assumptions:

1. they represent volume fractions:

$$\beta_j \in [0,1], \quad j \in \{1,2,3,4\}$$

2. no void can appear in the mixture and no phases interpenetration occurs:

$$\beta_1 + \beta_2 + \beta_3 + \beta_4 = 1$$

3. the austenite volume fraction cannot increase with respect to its initial value at time $\tau = 0$:

$$\beta_1 \le \beta_1^{in}$$

Under these assumptions, vector $\boldsymbol{\beta} = (\beta_1, \beta_2, \beta_3)$ univocally describes alloy composition because of $\beta_4 = 1 - \beta_1 - \beta_2 - \beta_3$. Accordingly, the state quantities for describing the 1D pseudoelastic behavior of SMAs are chosen as

$$S = \{\varepsilon_e, \varepsilon_i, \boldsymbol{\beta}\} \tag{2}$$

Reference state is defined in terms of state quantities values (that is, $\bar{\varepsilon}_e$, $\bar{\varepsilon}_i$, and $\bar{\boldsymbol{\beta}}$ at time $\tau = \bar{t}$) and state quantities evolutions (that is, $\dot{\bar{\varepsilon}}_e$, $\dot{\bar{\varepsilon}}_i$, and $\dot{\bar{\boldsymbol{\beta}}}$ in the sense of left-derivative with respect to reference time $\tau = \bar{t}$, with $d\bar{\varepsilon}_e = \dot{\bar{\varepsilon}}_e dt$, $d\bar{\varepsilon}_i = \dot{\bar{\varepsilon}}_i dt$, and $d\bar{\boldsymbol{\beta}} = \dot{\bar{\boldsymbol{\beta}}} dt$).
Introducing the convex set

$$C := \{\mathbf{x} = (x_1, x_2, x_3)^t \in \mathbb{R}^3 \,|\, x_1, x_2, x_3 \in [0,1], x_1 + x_2 + x_3 \le 1, x_1 \le x_1^{in}\} \tag{3}$$

physical restrictions in **Ass. 1**, **Ass. 2** and **Ass. 3** can be summarized as

$$\boldsymbol{\beta} \in C \tag{4}$$

The ideal pseudo-elastic behavior will be described by introducing few model parameters that can be straightforwardly obtained from experiments:

- direct and reverse transformation stresses $\sigma_{d/r}^{+/-} = \sigma_{d/r}^{+/-}(T)$;
- direct and reverse transformation strains $\varepsilon_{D/R}^{+/-} = \varepsilon_{D/R}^{+/-}(T)$;
- Young's modulus E_j of the j^{th} alloy phase, assumed to be isotropic linearly elastic.

Parameters with the same physical meaning are introduced in many SMA available models [1, 4, 5, 9], and thereby can be retained as classical. Nevertheless, the possibility to address the non-linear dependence of transformation strains and stresses on temperature is a novelty with respect to most well-established available models, in agreement with the improvements proposed by Lagoudas and co-workers, [14]. It is worth pointing out that present approach does not require to fix an *a-priori* specific form for the interpolation function describing the non-linear dependence of $\sigma_{d/r}^{+/-}$ and $\varepsilon_{D/R}^{+/-}$ on T.

Flow rule

The difference between austenite and single-variant martensite is quite small: while the unit cell of austenite is, on average, a perfect cube, the transformation to martensite distorts this cube by interstitial carbon atoms. Addressing an uniaxial traction, the unit cell after the transformation can be phenomenologically described as slightly longer in the traction direction and shorter in the orthogonal directions. Since multi-variant martensite is a mixture of single-variant configurations, the same can be said for the transformation from non-sheared to sheared lattice configurations in the martensitic phase.
In the present one-dimensional framework, the atomic rearrangement occurring during the transformation A/Mm $\leftrightarrow$ Ms+/Ms- is herein kinematically described via a phenomenological way by introducing $\dot{\varepsilon}^{ori}$ as the elongation-rate of the unit cell, herein defined as

$$\dot{\varepsilon}^{ori} = \dot{\varepsilon}^{ori}(\dot{\varepsilon}, d\boldsymbol{\beta}) := [H(|d\beta_2|) + H(|d\beta_3|)]\dot{\varepsilon}, \tag{5}$$

where $H(x)$ denotes the Heaviside function (such that $H(x) = 0$ for $x \le 0$ and $H(x) = 1$ for $x > 0$). Results will show that $\dot{\varepsilon}^{ori} \le \dot{\varepsilon}$ because, thanks to modeling choices, the onset of transformations will never simultaneously imply $d\beta_2 \ne 0$ and $d\beta_3 \ne 0$.

Equilibrium equations and constitutive laws

Denoting virtual quantities with the hat superscript and introducing $\{\sigma_e, \sigma_i, \mathbf{b}\}$ as the set of interior forces dual to S, the increment of virtual work density for external and internal actions are

$$dw_{ext}(d\hat{\varepsilon}) = \sigma d\hat{\varepsilon}, \qquad dw_{int}(d\hat{\varepsilon}_e, d\hat{\varepsilon}_i, d\hat{\boldsymbol{\beta}}) = \sigma_e d\hat{\varepsilon}_e + \sigma_i d\hat{\varepsilon}_i + \mathbf{b} \cdot d\hat{\boldsymbol{\beta}}$$

By employing the Principle of Virtual Work ($dw_{int} = dw_{ext}$ for any $d\hat{\varepsilon} = d\hat{\varepsilon}_e + d\hat{\varepsilon}_i$ and for any $d\hat{\boldsymbol{\beta}}$), the arbitrariness of virtual quantities $d\hat{\varepsilon}_e$, $d\hat{\varepsilon}_i$, and $d\hat{\boldsymbol{\beta}}$ gives the equilibrium relationships:

$$\sigma_e = \sigma_i = \sigma, \qquad \mathbf{b} = 0 \tag{6}$$

Interior forces are split in non-dissipative (denoted by the superscript *nd*) and dissipative terms (superscript *d*). The constitutive laws are chosen by introducing the free-energy $\Psi = \Psi(S)$ (providing the non-dissipative terms) and the pseudo-potential of dissipation $\Phi = \Phi(\dot{S})$ (providing the dissipative ones),

$$\sigma_e = \sigma_e^{nd} + \sigma_e^{d} = \frac{\partial \Psi}{\partial \varepsilon_e} + \frac{\partial \Phi}{\partial \dot{\varepsilon}_e}, \quad \sigma_i = \sigma_i^{nd} + \sigma_i^{d} = \frac{\partial \Psi}{\partial \varepsilon_i} + \frac{\partial \Phi}{\partial \dot{\varepsilon}_i}, \quad \mathbf{b} = \mathbf{b}^{nd} + \mathbf{b}^{d} = \frac{\partial \Psi}{\partial \boldsymbol{\beta}} + \frac{\partial \Phi}{\partial \dot{\boldsymbol{\beta}}} \tag{7}$$

The free-energy Ψ of the alloy is chosen as:

$$\Psi(\varepsilon_e, \boldsymbol{\beta}) := \Psi_{el}(\varepsilon_e) + \Psi_{ch}(\boldsymbol{\beta}) \tag{8}$$

where:

- Ψ_{el} is the elastic free-energy contribution:

$$\Psi_{el}(\varepsilon_e) := \bar{\Psi}_{el} + \bar{\sigma} : d\varepsilon_e + \frac{1}{2}\sum_{j=1}^{4} \bar{\beta}_j E_j d\varepsilon_e : d\varepsilon_e$$

where $\bar{\sigma}$ and $\bar{\Psi}_{el}$ are the reference values at $\tau = \bar{t}$ of Cauchy stress and elastic free-energy, respectively. Assuming an undeformed material at the initial configuration, then it results $\bar{\sigma} = \bar{\Psi}_{el} = 0$ at $\tau = 0$.

- Ψ_{ch} is the free-energy contribution, related to the phase change:

$$\Psi_{ch}(\boldsymbol{\beta}) := -\boldsymbol{\beta} \cdot \mathbf{r}(\bar{\varepsilon}, \bar{\sigma}, \bar{\boldsymbol{\beta}}) + \mathrm{I}_C(\boldsymbol{\beta})$$

where the indicator function I_C ensures condition (4) to be satisfied. Moreover, $\mathbf{r}$ represents the phase transformation rate vector, defined as:

$$\mathbf{r}(x, y, \mathbf{v}) := \begin{pmatrix} g_a(y, \mathbf{v}) \\ g_+(y, \mathbf{v}) \\ g_-(y, \mathbf{v}) \end{pmatrix} |x|, \qquad \text{with } x, y \in \mathbb{R}, \mathbf{v} = (v_1, v_2, v_3)^t \in \mathbb{R}^3$$

Phase change activates on the basis of temperature and stress states, being here regulated by activation functions:

$$g_+(y, \mathbf{v}) := [1 - H(v_3)]H(y - \sigma_d^+)/\varepsilon_D^+ - H(v_2)H(-y + \sigma_r^+)/\varepsilon_R^+$$

$$g_-(y, \mathbf{v}) := [1 - H(v_2)]H(-y + \sigma_d^-)/\varepsilon_D^- - H(v_3)H(y - \sigma_r^-)/\varepsilon_R^-$$

$$g_a(y, \mathbf{v}) := -g_+(y, \mathbf{v}) - g_-(y, \mathbf{v})$$

Transformation strains $\varepsilon_{D/R}^{+/-}$ as well as transformation stresses $\sigma_{d/r}^{+/-}$ depend on temperature T and they can be straight obtained from experimental data, as reported in Fig. 1. Since present work addresses isothermal conditions, transformation stresses and strains are here fixed parameters. Nevertheless, when non-isothermal conditions are addressed, values of transformation stresses and strains at the reference temperature $\bar{T}$ (at $\tau = \bar{t}$) can be considered.
The pseudo-potential of dissipation Φ is chosen as:

$$\Phi(\dot{\varepsilon}_i, \dot{\boldsymbol{\beta}}) := \Phi_{ch}(\dot{\boldsymbol{\beta}}) + \Phi_{fr}(\dot{\varepsilon}_i) \tag{9}$$

where:

- Φ_{ch} is the pseudo-potential of dissipation related to the phase change:

$$\Phi_{ch}(\dot{\boldsymbol{\beta}}) := \frac{\|\dot{\boldsymbol{\beta}}\|^2}{2}$$

- Φ_{fr} is the pseudo-potential of dissipation related to the flow rule:

$$\Phi_{fr}(\dot{\varepsilon}_i) := \mathrm{I}_o(\dot{\varepsilon}_i - \bar{\dot{\varepsilon}}^{ori})$$

with I_o the indicator function of the zero value and $\bar{\dot{\varepsilon}}^{ori} := \dot{\varepsilon}^{ori}(\bar{\varepsilon}, d\bar{\boldsymbol{\beta}})$.

It is worth pointing out that dimensional multiplicative unitary coefficients have to be considered in previous relationships, when necessary, in order to respect the unit of measure of the free-energy (namely, work per unit volume) and of the pseudo-potential of dissipation (that is, power per unit volume). These coefficients have been omitted here for the sake of compactness.

Accordingly, since derivation with respect to a finite quantity (for instance, ε_e) is formally equivalent to the one with respect to a perturbation (for instance, $d\varepsilon_e$), constitutive choices (7), (8), and (9) give the interior forces as equal to:

$$\sigma_e = \bar{\sigma} + \sum_{j=1}^{4} \bar{\beta}_j E_j d\varepsilon_e \qquad \sigma_i \in \partial \mathrm{I}_o(\dot{\varepsilon}_i - \bar{\dot{\varepsilon}}^{ori}) \tag{10}$$

$$\dot{\boldsymbol{\beta}} - \mathbf{r}(\bar{\dot{\varepsilon}}, \bar{\sigma}, \bar{\boldsymbol{\beta}}) + \partial \mathrm{I}_C(\boldsymbol{\beta}) \ni \mathbf{0} \tag{11}$$

Governing equations

Assuming strain ε as control variable, the governing equations of the SMA thermodynamical problem, obtained from equilibrium relationships (6) and constitutive choices (7), (8), and (9), give the evolution of stress σ and alloy composition $\boldsymbol{\beta}$. Stress σ results from:

$$\sigma = \bar{\sigma} + \sum_{j=1}^{4} \bar{\beta}_j E_j d\varepsilon_e \quad \text{with} \quad d\varepsilon_e = d\varepsilon - d\varepsilon_i, \quad d\varepsilon_i = (H(|\, d\bar{\beta}_2\,|) + H(|\, d\bar{\beta}_3\,|))d\bar{\varepsilon} \tag{12}$$

Alloy composition $\boldsymbol{\beta}$ is found by means of a single-step prediction-projection procedure. Tentative values of volume fractions $\breve{\beta}_j = \bar{\beta}_j + d\breve{\beta}_j$ (with $j = 1,2,3$) are computed first, where:

$$d\breve{\beta}_1 = -d\breve{\beta}_2 - d\breve{\beta}_3 \tag{13}$$

$$d\breve{\beta}_2 = \{[1 - H(\bar{\beta}_3)]H(\bar{\sigma} - \sigma_d^+)/\varepsilon_D^+ - H(\bar{\beta}_2)H(-\bar{\sigma} + \sigma_r^+)/\varepsilon_R^+\}\,|\,d\bar{\varepsilon}\,| \tag{14}$$

$$d\breve{\beta}_3 = \{[1 - H(\bar{\beta}_2)]H(-\bar{\sigma} + \sigma_d^-)/\varepsilon_D^- - H(\bar{\beta}_3)H(\bar{\sigma} - \sigma_r^-)/\varepsilon_R^-\}\,|\,d\bar{\varepsilon}\,| \tag{15}$$

and then $\boldsymbol{\beta}$ is obtained as

$$\boldsymbol{\beta} = \begin{cases} \breve{\boldsymbol{\beta}} = (\breve{\beta}_1, \breve{\beta}_2, \breve{\beta}_3)^t & \text{if } \breve{\boldsymbol{\beta}} \in C \\ \boldsymbol{\beta}^{pr} & \text{if } \breve{\boldsymbol{\beta}} \notin C \end{cases}, \tag{16}$$

being $\boldsymbol{\beta}^{pr} = (\beta_1^{pr}, \beta_2^{pr}, \beta_3^{pr})^t$ the orthogonal projection of $\breve{\boldsymbol{\beta}}$ on C. Finally, it is worth pointing out that constitutive choices in Eq. (7) and the convexity of the pseudo-potential of dissipation in Eq. (9) allow to *a-priori* satisfy the inequality constraint prescribed by the second law of thermodynamics, [15-17].

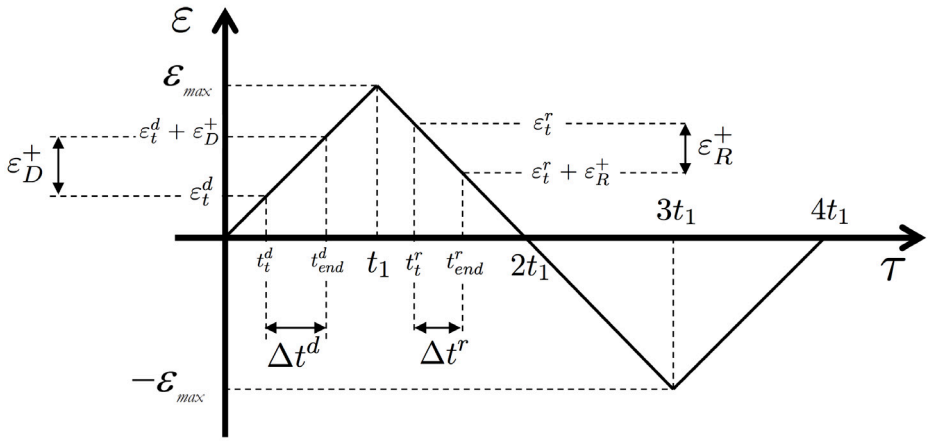

Figure 2: Applied strain ε vs. time τ.

RESULTS

A loading-unloading displacement-based uniaxial test at constant temperature T is simulated. Starting from $\varepsilon = 0$, a constant strain-rate $|\dot{\varepsilon}| = \dot{e}$ is applied with maximum and minimum strain ε_{max} and $-\varepsilon_{max}$, respectively. Accordingly, introducing $t_1 = \varepsilon_{max} / \dot{e}$, applied strain-time law is (see Fig. 2).

$$\varepsilon = \varepsilon(\tau) = \begin{cases} \dot{e}\tau & \text{for} \quad \tau = [0, t_1] \\ -\dot{e}\tau + 2\varepsilon_{max} & \text{for} \, \tau = (t_1, 3t_1] \\ \dot{e}\tau - 4\varepsilon_{max} & \text{for} \, \tau = (3t_1, 4t_1] \end{cases} \tag{17}$$

Therefore, the material element is loaded for $\tau \in [0, t_1]$ and $\tau \in [2t_1, 3t_1]$, while unloading conditions are addressed for $\tau \in [t_1, 2t_1]$ and $\tau \in [3t_1, 4t_1]$.

Two cases are preliminary distinguished: the high-temperature response for $T > T_{af}$ and the low-temperature one for $T < T_{mf}$. Accordingly, in the former case, the alloy is fully austenitic (that is, $\beta_1^{in} = 1$), while in the latter the alloy is characterized by a multi-variant martensitic lattice arrangement (namely, $\beta_4^{in} = 1$). Moreover, the response of the model at $T_{mf} < T < T_{af}$, where the co-existence of multi-variant martensite and austenite is admissible, is described. Finally, relationships for setting the value of reverse transformation strains in function of experimental residual strains are given.

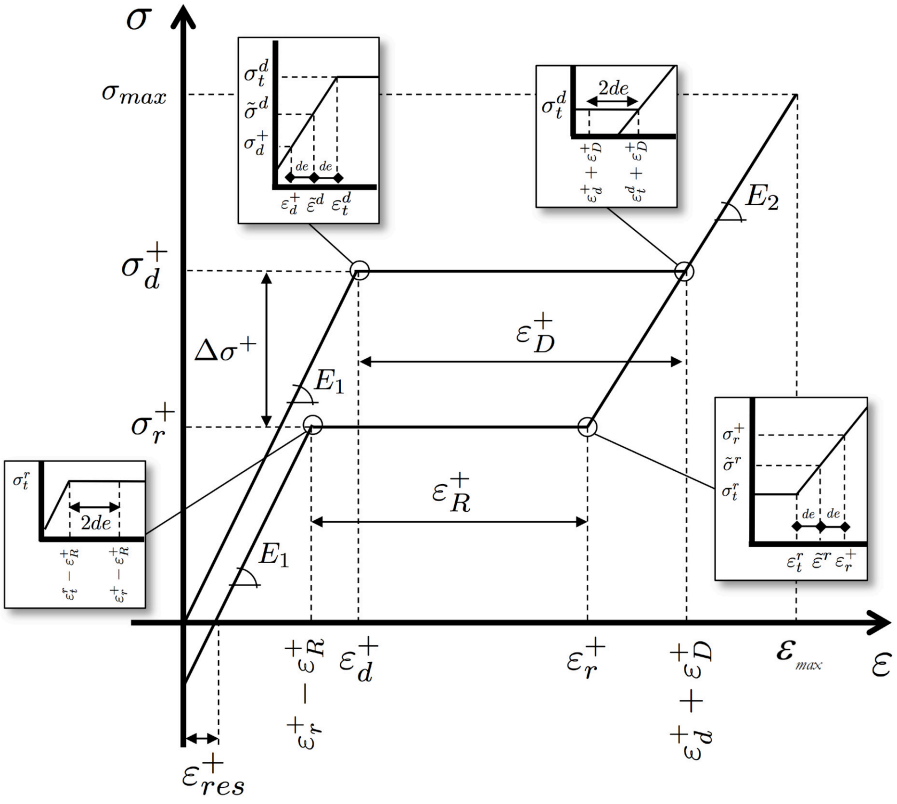

Figure 3: Stress σ vs. strain ε predicted by present model in a displacement-driven traction loading-unloading test at the high temperature $T_2 > T_{af}$. The applied strain is depicted in Fig. 2 for $\tau \in [0, 2t_1]$.

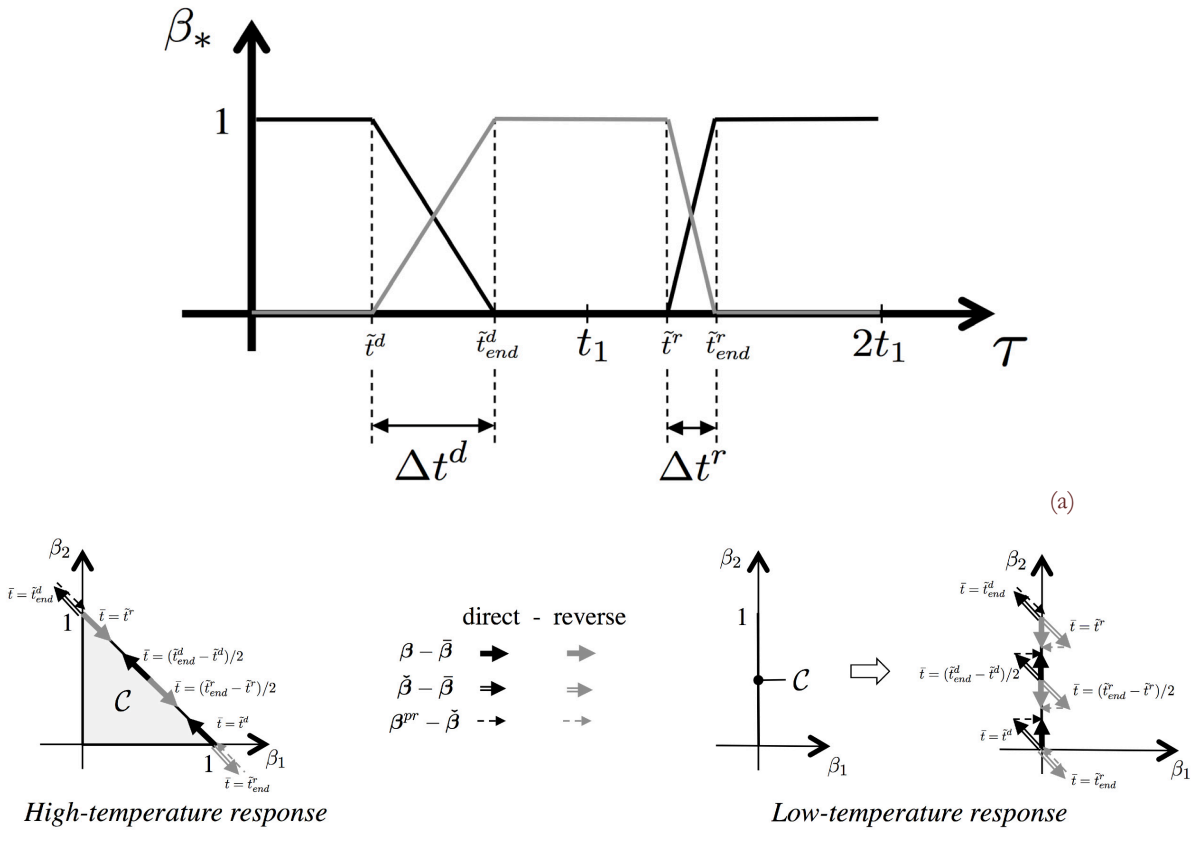

Figure 4: Alloy composition predicted by present model for a traction loading-unloading test obtained from applied strain in Fig. 2 for $\tau \in [0, 2t_1]$. (a) In black, β_1 (resp., β_4) vs. τ at the high temperature T_2 (resp., low temperature T_1); in grey, β_2 vs. τ. (b) Evolution of alloy composition in the space of the admissible volume fractions at high and low temperature (dimensions of arrows are not in scale).

High-temperature response

The stress-strain relationship as well as the alloy composition predicted by present model at high temperature are obtained by construction, considering different time intervals.

Traction loading-unloading: $\tau \in [0, 2t_1]$. For presenting a detailed description of analytical results and denoting with $de = \dot{e}dt$, it is assumed that there exists natural numbers $K_1, K_2, K_3, K_4 >> 1$ such that $E_1 K_1 de = \sigma_d^+$, $K_2 de = \varepsilon_R^+$, $\sigma_d^+ - E_2 K_3 de = \sigma_r^+$, and $K_4 de = \varepsilon_R^-$. Obtained results in terms of SMA stress-strain relationship and alloy composition are described in the following and are reported in Figs. 3 and 4.

Traction loading. For $\tau \in [0, t_1]$, the material element is loaded with $d\varepsilon = de = \dot{e}dt$. For the sake of notation, let introduce the following stress and strain values:

$$\tilde{\sigma}^d = \sigma_d^+ + E_1 de, \quad \tilde{\varepsilon}^d = \frac{\tilde{\sigma}^d}{E_1}$$

the time interval $\Delta t^d = \varepsilon_D^+ / \dot{e}$, and the time values:

$$\tilde{t}^d = \frac{\tilde{\varepsilon}^d}{\dot{e}}, \quad t_t^d = \tilde{t}^d + dt, \quad \tilde{t}_{end}^d = \tilde{t}^d + \Delta t^d, \quad t_{end}^d = t_t^d + \Delta t^d \tag{18}$$

where $t_{end}^d < t_1$ is assumed. Model predicts the following response:

• $\bar{t} \in [0, \tilde{t}^d)$. At each step, it results $d\bar{\beta}_2 = d\bar{\beta}_3 = 0$ and thereby Eq. (12) gives $d\varepsilon_i = 0$, $d\varepsilon_e = de$, $\sigma = \bar{\sigma} + E_1 de \le \sigma_d^+$. Hence, from Eq. (13-15) and (16), it results $\boldsymbol{\beta} = \bar{\boldsymbol{\beta}} = \boldsymbol{\beta}^{in}$.

• $\bar{t} = \tilde{t}^d$. It results $\bar{\varepsilon} = \tilde{\varepsilon}^d$ and $\bar{\sigma} = \tilde{\sigma}^d > \sigma_d^+$, and thereby Eq. (13-15) and (16) give (since $\bar{\beta}_2 = 0$)

$$\mathbf{r}(\bar{\dot{\varepsilon}}, \bar{\sigma}, \bar{\boldsymbol{\beta}}) = \begin{pmatrix} -\dot{e} / \varepsilon_D^+ \\ \dot{e} / \varepsilon_D^+ \\ 0 \end{pmatrix} \Rightarrow \begin{cases} d\breve{\beta}_1 = -de / \varepsilon_D^+ \\ d\breve{\beta}_2 = de / \varepsilon_D^+ \\ d\breve{\beta}_3 = 0 \end{cases} \Rightarrow \begin{cases} \breve{\beta}_1 = \bar{\beta}_1 - de / \varepsilon_D^+ \\ \breve{\beta}_2 = \bar{\beta}_2 + de / \varepsilon_D^+ \\ \breve{\beta}_3 = 0 \end{cases} \tag{19}$$

Accordingly, it results $\breve{\boldsymbol{\beta}} = (1 - de / \varepsilon_D^+, de / \varepsilon_D^+, 0)^t \in C$ and $\boldsymbol{\beta}(\tilde{t}) = \breve{\boldsymbol{\beta}}$ (see Fig. 4). Thereby, stress $\tilde{\sigma}^d$ and the corresponding strain $\tilde{\varepsilon}^d$ denote reference stress and strain values at the onset of the direct transformation. Moreover, from Eq. (12) and since $d\bar{\beta}_2 = d\bar{\beta}_3 = 0$, it results $d\varepsilon_i = 0$, $d\varepsilon_e = de$, and $\sigma = \bar{\sigma} + E_1 de = \sigma_t^d$. Accordingly, $\sigma_t^d = \tilde{\sigma}^d + E_1 de$ and $\varepsilon_t^d = \tilde{\varepsilon}^d + de$ are the starting stress and the starting strain of the direct transformation, respectively.

• $\bar{t} \in [t_t^d, t_{end}^d)$. At each step, it results $d\bar{\beta}_2 > 0$ and $d\bar{\beta}_3 = 0$, and thereby Eq. (12) gives $d\varepsilon_i = de$, $d\varepsilon_e = 0$, and $\sigma = \bar{\sigma} = \sigma_t^d$. Accordingly, a plateau in the stress-strain response is obtained during the martensitic orientation that occurs at the direct transformation stress σ_t^d (see Fig. 3). During the overall transformation, the evolution laws for the volume fractions result in $\dot{\beta}_1 = -\dot{\beta}_2 = -\dot{e} / \varepsilon_D^+$ as long as $\bar{\beta}_2 < 1$ (and thereby $\bar{\beta}_1 > 0$). Accordingly, a complete direct martensitic transformation (corresponding to β_2 going from 0 to 1) is obtained in the time interval Δt^d (see Fig. 4).
Thereby, time $\bar{t} = t_{end}^d - dt = \tilde{t}_{end}^d$ corresponds to $\bar{\beta}_2 = 1$ and $\bar{\beta}_1 = 0$ (but $d\bar{\beta}_2 > 0$ and $d\bar{\beta}_3 = 0$), or, in other words, to a complete direct transformation. In this situation and as shown in Fig. 4, variations of tentative volume fractions are the same as in Eq. (19), and Eq. (16) gives

$$\breve{\boldsymbol{\beta}} = \begin{pmatrix} -de / \varepsilon_D^+ \\ 1 + de / \varepsilon_D^+ \\ 0 \end{pmatrix} \Rightarrow \breve{\boldsymbol{\beta}} \notin C \Rightarrow \boldsymbol{\beta} = \boldsymbol{\beta}^{pr} = \begin{pmatrix} 0 \\ 1 \\ 0 \end{pmatrix} \tag{20}$$

Moreover, actual strain is $\varepsilon = \varepsilon_t^d + \varepsilon_D^+$, with the strain produced during the martensitic lattice orientation being fully inelastic, and equal to $\varepsilon_i = \varepsilon_D^+$ (see Fig. 3).

• $\bar{t} \in [t_{end}^d, t_1]$. At each step, alloy composition is governed by the projection described in Eq. (20). It results $d\bar{\beta}_2 = d\bar{\beta}_3 = 0$, and thereby Eq. (12) gives $d\varepsilon_e = de$, $d\varepsilon_i = 0$, and $\sigma = \sigma_t^d + E_2(\varepsilon - \varepsilon_D^+ - \varepsilon_t^d)$ (see Fig. 3).
Traction unloading. For $\tau \in [t_1, 2t_1]$, the material element undergoes unloading conditions (in fact, $d\varepsilon = -de$). Consider the following relevant stress and strain values:

$$\tilde{\sigma}^r = \sigma_r^+ - E_2 de = \sigma_r^+ - E_2 de - \sigma_d^+ + \sigma_d^+ + E_1 de - E_1 de = \tilde{\sigma}^d - \Delta\sigma^+, \qquad \tilde{\varepsilon}^r = \frac{\sigma_{max} - \tilde{\sigma}^r}{E_2}$$

with $\Delta\sigma^+ = \sigma_d^+ - \sigma_r^+ + (E_1 + E_2) de$ and $\sigma_{max} = \sigma_t^d + E_2(\varepsilon_{max} - \varepsilon_D^+ - \varepsilon_t^d)$. Moreover, let introduce the time interval $\Delta t^r = \varepsilon_R^+ / \dot{e}$ and the time values:

$$\tilde{t}^r = \frac{\varepsilon_{max} - \tilde{\varepsilon}^r}{\dot{e}}, \quad t_t^r = \tilde{t}^r + dt, \quad \tilde{t}_{end}^r = \tilde{t}^r + \Delta t^r, \quad t_{end}^r = t_t^r + \Delta t^r \tag{21}$$

where $t_{end}^r < 2t_1$ is assumed. Model predictions are as follows:

• $\bar{t} \in (t_1, \tilde{t}^r)$. At each step, it results $d\bar{\beta}_2 = d\bar{\beta}_3 = 0$, and thereby Eq. (12) gives $d\varepsilon_i = 0$, $d\varepsilon_e = -de$, $\sigma = \bar{\sigma} - E_2 de \ge \sigma_r^+$. Accordingly, it results $\boldsymbol{\beta} = \bar{\boldsymbol{\beta}} = (0,1,0)^t$. In fact, if $\bar{\sigma} > \sigma_d^+$, volume fractions follow Eq. (20). Otherwise, if $\bar{\sigma} \le \sigma_d^+$, from Eq. (13-15) it results $d\breve{\beta}_1 = d\breve{\beta}_2 = d\breve{\beta}_3 = 0$.

- $\bar{t} = \tilde{t}^r$. It results $\bar{\varepsilon} = \tilde{\varepsilon}^r$ and $\bar{\sigma} = \tilde{\sigma}^r < \sigma_r^+$, and Eq. (13-15) give (since $\bar{\beta}_2 = 1$ and $\bar{\beta}_3 = 0$)

$$\mathbf{r}(\dot{\bar{\varepsilon}}, \bar{\sigma}, \bar{\boldsymbol{\beta}}) = \begin{pmatrix} \dot{e} / \varepsilon_R^+ \\ -\dot{e} / \varepsilon_R^+ \\ 0 \end{pmatrix} \Rightarrow \begin{cases} d\breve{\beta}_1 = de / \varepsilon_R^+ \\ d\breve{\beta}_2 = -de / \varepsilon_R^+ \\ d\breve{\beta}_3 = 0 \end{cases} \Rightarrow \begin{cases} \breve{\beta}_1 = de / \varepsilon_R^+ \\ \breve{\beta}_2 = 1 - de / \varepsilon_R^+ \\ \breve{\beta}_3 = 0 \end{cases} \tag{22}$$

resulting $\breve{\boldsymbol{\beta}} \in C$ and thereby $\boldsymbol{\beta} = \breve{\boldsymbol{\beta}}$ from Eq. (16). Accordingly, stress $\tilde{\sigma}^r$ and the corresponding strain $\tilde{\varepsilon}^r$ denote reference stress and strain values at the onset of the reverse transformation. Moreover, from Eq. (12) and since $d\bar{\beta}_2 = d\bar{\beta}_3 = 0$, it results $d\varepsilon_i = 0$, $d\varepsilon_e = de$, and $\sigma = \bar{\sigma} - E_2 de = \sigma_t^r$. Accordingly, $\sigma_t^r = \tilde{\sigma}^r - E_2 de$ and $\varepsilon_t^r = \tilde{\varepsilon}^r - de$ are the starting stress and the starting strain of the reverse transformation.

- $\bar{t} \in [t_t^r, t_{end}^r)$. At each step, it results $d\bar{\beta}_2 < 0$ and $d\bar{\beta}_3 = 0$, and thereby Eq. (12) gives $d\varepsilon_i = -de$, $d\varepsilon_e = 0$, and $\sigma = \bar{\sigma} = \sigma_t^r$. Accordingly, a plateau in the stress-strain response is obtained during the martensitic de-orientation, occurring at the reverse transformation stress σ_t^r. During the overall transformation, the evolution laws for the volume fractions result in $\dot{\beta}_1 = -\dot{\beta}_2 = \dot{e} / \varepsilon_R^+$ as long as $\bar{\beta}_2 > 0$ (and thereby $\bar{\beta}_1 < 1$). Accordingly, a complete reverse martensitic transformation (corresponding to β_2 going from 1 to 0) is obtained in the time interval Δt^r.

Thereby, time $\bar{t} = \tilde{t}_{end}^r = t_{end}^r - dt$ corresponds to $\bar{\beta}_1 = 1$ and $\bar{\beta}_2 = 0$ (but $d\bar{\beta}_2 < 0$ and $d\bar{\beta}_3 = 0$) or, in other words, to a complete reverse transformation. In this situation, variations of the tentative volume fractions and alloy compositions are obtained from Eq. (13-15) and (16), and therefore

$$\begin{cases} d\breve{\beta}_1 = de / \varepsilon_R^+ \\ d\breve{\beta}_2 = -de / \varepsilon_R^+ \\ d\breve{\beta}_3 = 0 \end{cases} \Rightarrow \breve{\boldsymbol{\beta}} = \begin{pmatrix} 1 + de / \varepsilon_R^+ \\ -de / \varepsilon_R^+ \\ 0 \end{pmatrix} \notin C \Rightarrow \boldsymbol{\beta} = \boldsymbol{\beta}^{br} = \begin{pmatrix} 1 \\ 0 \\ 0 \end{pmatrix} \tag{23}$$

Moreover, actual strain is $\varepsilon = \varepsilon_t^r - \varepsilon_R^+$, with the strain produced during the martensitic lattice de-orientation (during the time interval $\tau \in [t_t^r, t_{end}^r]$) being fully inelastic and equal to $\varepsilon_i = -\varepsilon_R^+$. Accordingly, considering a complete loading-unloading cycle (that is, $\tau \in [0, t_{end}^r]$), the total inelastic strain at the end of the test is $\varepsilon_D^+ - \varepsilon_R^+$.

- $\bar{t} \in [t_{end}^r, 2t_1]$. At each step, alloy composition is governed by the projection described in Eq. (23). It results $d\bar{\beta}_2 = d\bar{\beta}_3 = 0$, and thereby Eq. (12) gives $d\varepsilon_e = -de$, $d\varepsilon_i = 0$, and $\sigma = \bar{\sigma} - E_1 de$.

It is worth pointing out that, in the limit $dt \to 0$, it results

$$\sigma_t^d \to \tilde{\sigma}^d \to \sigma_d^+, \quad \varepsilon_t^d \to \tilde{\varepsilon}^d \to \varepsilon_d^+, \quad \sigma_t^r \to \tilde{\sigma}^r \to \sigma_r^+, \quad \varepsilon_t^r \to \tilde{\varepsilon}^r \to \varepsilon_r^+, \quad \Delta\sigma^+ \to \sigma_d^+ - \sigma_r^+$$

where $\varepsilon_d^+ = \sigma_d^+ / E_1$ and $\varepsilon_r^+ = \sigma_d^+ / E_1 + \varepsilon_D^+ - \Delta\sigma^+ / E_2$. In summary, in the limit $dt \to 0$, the obtained constitutive relationship during a tensile traction-release test is (see Fig. 3)

$$\text{Loading } \varepsilon \in [0, \varepsilon_{\max}] : \sigma(\varepsilon) \to \begin{cases} E_1 \varepsilon & \text{if } \varepsilon \le \varepsilon_d^+ \\ \sigma_d^+ & \text{if } \varepsilon_d^+ < \varepsilon \le \varepsilon_d^+ + \varepsilon_D^+ \\ \sigma_d^+ + E_2(\varepsilon - \varepsilon_D^+ - \varepsilon_d^+) & \text{if } \varepsilon > \varepsilon_d^+ + \varepsilon_D^+ \end{cases} \tag{24}$$

$$\text{Unloading } \varepsilon \in [\varepsilon_{\max}, 0] : \sigma(\varepsilon) \to \begin{cases} \sigma_d^+ + E_2(\varepsilon - \varepsilon_D^+ - \varepsilon_d^+) & \text{if } \varepsilon > \varepsilon_r^+ \\ \sigma_r^+ & \text{if } \varepsilon_r^+ - \varepsilon_R^+ < \varepsilon \le \varepsilon_r^+ \\ E_1 \varepsilon & \text{if } \varepsilon \le \varepsilon_r^+ - \varepsilon_R^+ \end{cases} \tag{25}$$

and the corresponding evolution of single-oriented martensitic microstructure β_2 is

$$\text{Loading } \varepsilon \in [0,\varepsilon_{\max}]: \beta_2(\varepsilon) \rightarrow \begin{cases} 0 & \text{if} \quad \varepsilon \le \varepsilon_d^+ \\ \dfrac{\varepsilon - \varepsilon_d^+}{\varepsilon_D^+} & \text{if} \quad \varepsilon_d^+ < \varepsilon \le \varepsilon_d^+ + \varepsilon_D^+ \\ 1 & \text{if} \quad \varepsilon > \varepsilon_d^+ + \varepsilon_D^+ \end{cases} \tag{26}$$

$$\text{Unloading } \varepsilon \in [\varepsilon_{\max},0]: \beta_2(\varepsilon) \rightarrow \begin{cases} 1 & \text{if} \quad \varepsilon > \varepsilon_r^+ \\ \dfrac{\varepsilon_r^+ - \varepsilon}{\varepsilon_R^+} & \text{if} \quad \varepsilon_r^+ - \varepsilon_R^+ < \varepsilon \le \varepsilon_r^+ \\ 0 & \text{if} \quad \varepsilon \le \varepsilon_r^+ - \varepsilon_R^+ \end{cases} \tag{27}$$

with $\beta_1(\varepsilon) = 1 - \beta_2(\varepsilon)$. The behavior of the alloy, as obtained from Eq. (24-27), is fully strain-rate independent. Moreover, due to the phase diagram in Fig. 1, reverse transformation occurs at positive stresses at high-temperature (namely, $\sigma_r^+(T) > 0$ for $T > T_{r0}$), reproducing the characteristic pseudo-elastic behavior of SMAs in initial austenitic microstructure.

Compression loading-unloading: $\tau \in [2t_1, 4t_1]$. In this case, the behavior of the alloy in terms of the stress-strain relationship and alloy composition is analogous to the traction behavior. In fact, it can be obtained from previous relationships by replacing β_2 with β_3, ε_D^+ with ε_D^-, ε_R^+ with ε_R^-, σ_d^+ with σ_d^-, σ_r^+ with σ_r^-. It is worth pointing out that, in the compressive regime, $d\varepsilon = -de$ is associated with loading conditions, and $d\varepsilon = de$ with un-loading ones.

The full SMA stress-strain constitutive response, obtained by addressing the traction-compression loading-unloading cycle in Eq. (17) for $\tau \in [0, 4t_1]$ at high temperature $T_2 > T_{af} > T_{m}$, is depicted in Fig. 5a.

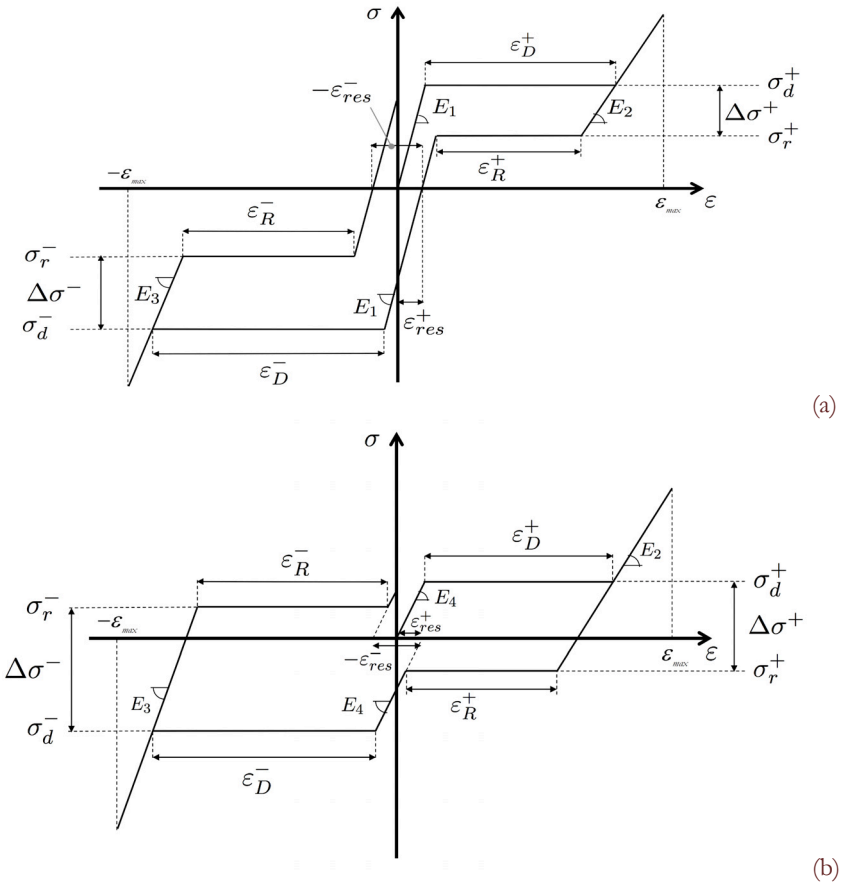

Figure 5: Stress σ vs. strain ε predicted by present model in a tensile-compressive loading-unloading test obtained from applied strain as in Fig. 2 at the high temperature T_2 (a) and at the low temperature T_1 (b).

Low-temperature response

Despite the low-temperature response of SMAs is very different from the high-temperature one, analytical relationships obtained via present model are only slightly different from the ones above described. Firstly, due to the multi-variant martensitic lattice arrangement of the alloy, Young's modulus E_4 should be employed instead of E_1.

When $\bar{\sigma} > \sigma_d^+$, the onset of the direct transformation occurs and the tentative alloy composition is the same as in Eq. (19) but, since $\beta_1^{in} = 0$, it results $\breve{\boldsymbol{\beta}} \notin C$ and Eq. (16) gives $\boldsymbol{\beta} = \boldsymbol{\beta}^{pr} = (0, de/\varepsilon_D^+, 0)^t$ with $\beta_4 = 1 - de/\varepsilon_D^+$. This is clearly shown in Fig. 4, where it is also highlighted that analogous projection occurs during the overall direct transformation up to $\boldsymbol{\beta} = (0,1,0)^t$.

Similarly, model behavior is different also at the reverse transformation, where tentative volume fractions are given by Eq. (22) (identical to the high-temperature case), resulting now $\breve{\boldsymbol{\beta}} \notin C$. Thereby, as shown in Fig. 4, alloy composition at the onset of reverse transformation is obtained as $\boldsymbol{\beta} = \boldsymbol{\beta}^{pr} = (0, 1 - de/\varepsilon_D^+, 0)^t$ [see Eq. (16)] with $\beta_4 = de/\varepsilon_D^+$. Analogous projection occurs during the overall reverse transformation, up to $\boldsymbol{\beta} = (0,0,0)^t$ and $\beta_4 = 1$ (see Fig. 4).

The full SMA stress-strain constitutive response, obtained addressing the traction-compression loading-unloading cycle in Eq. (17) for $\tau \in [0, 4t_1]$ at the low temperature $T_1 < T_{mf} < T_{ro}$, is depicted in Fig. 5b. It is worth highlighting that the phase diagram in Fig. 1 determines that the reverse transformation occurs at negative stresses for low-temperature tests (for $T < T_{ro}$). Accordingly, in agreement with experimental evidence, no pseudo-elastic behavior appears at tensile stresses for SMAs in initial multi-variant martensitic microstructure.

Intermediate-temperature response

The model is able to deal with SMAs in an initial mixture composition characterized by both multi-variant martensite and austenite lattice arrangement, stable in the temperature range $T_{mf} < T < T_{af}$. The stress-strain constitutive relationship, obtained by addressing the traction-compression loading-unloading cycle in Eq. (17) for $\tau \in [0, 4t_1]$, is fully analogous to the ones reported in Fig. 5, but employing the transformation stresses values as from experimental phase diagram (see Fig. 1) and the initial Young's modulus $E^{in} = \beta_1^{in} E_1 + \beta_4^{in} E_4$ instead of E_1 and E_4. Nevertheless, as shown in Fig. 6 and due to the initial mixture composition, the evolution of phase volume fractions predicted by present model is significantly different from the ones obtained at high and low temperatures (see Fig. 4).

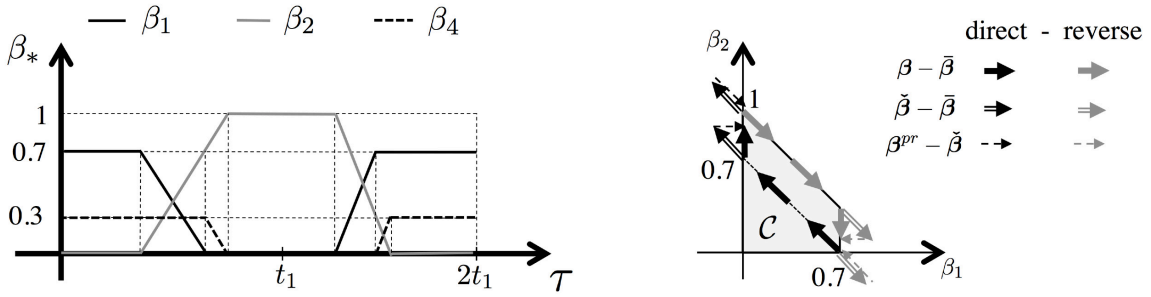

Figure 6: Alloy composition vs. time (left) and in the volume fraction space (right) predicted by present model for a traction loading-unloading test (see applied strain in Fig. 2 for $\tau \in [0, 2t_1]$) considering a SMA with initial mixture martensitic-austenitic composition with $\boldsymbol{\beta}^{in} = \boldsymbol{\beta}(0) = (0.7, 0, 0)^t$ (dimensions of arrows are not in scale).

Residual strains

Sometimes it can be easier to describe reverse transformation in terms of experimental data on residual strains ε_{res}^+ and ε_{res}^- instead of reverse transformation strains ε_R^+ and ε_R^-. By employing previous analytical results and addressing the traction-compression loading-unloading cycle as in Eq. (17), present model allows to derive useful relationships for setting the value of reverse transformation strains in order to obtain $\varepsilon = \varepsilon_{res}^+$ (resp., $\varepsilon = -\varepsilon_{res}^- - \varepsilon_{res}^+$) at $\sigma = 0$ at the end of the direct and reverse transformation cycle Mm/A $\leftrightarrow$ Ms+ (resp., Mm/A $\leftrightarrow$ Ms-),

$$\varepsilon_R^+ = \varepsilon_D^+ - \frac{(E^{in} - E_2)\Delta\sigma^+}{E^{in}E_2} - \varepsilon_{res}^+, \qquad \varepsilon_R^- = \varepsilon_D^- - \frac{(E^{in} - E_3)\Delta\sigma^-}{E^{in}E_3} - \varepsilon_{res}^- \tag{28}$$

where $\Delta\sigma^+ = \sigma_d^+ - \sigma_r^+$ and $\Delta\sigma^- = |\sigma_d^- - \sigma_r^-|$.

CONCLUSIONS

A novel constitutive model for the stress-induced martensitic transformations in SMAs has been proposed, accounting for: different behavior for the transformation laws of direct and reverse lattice rearrangement; asymmetric responses in tension and compression (both for transformation and stiffness properties); the possible co-existence of austenite, multi-variant and oriented martensites. Accordingly, the model is suitable for reproducing available experimental data on SMA pseudo-elastic properties.

The model is formulated in a generalized energetic framework. By introducing a suitable pseudo-potential of dissipation and by formulating transformation-evolution laws from microscopic equilibrium equations, the fulfillment of the second law of thermodynamics is *a-priori* satisfied, without the need of implicit algorithms. In order to highlight this feature, the model is developed in detail within a fully explicit framework, easy to be implemented for computational analyses. Obtained results clearly show this feature, highlighting that material parameter identification is straightforward from experimental data, even accounting for a possible non-perfect pseudo-elastic behavior for SMA.

The model has been here developed under the assumption of ideal non-hardening behavior. In upcoming works, it will be generalized in order to account for non-linear hardening effects, allowing for an effective comparison with experimental data. Moreover, shape-memory effects as well as non-isothermal response will be accounted for. Accordingly, the effects of non-linear transformation lines in the phase diagram, as well as of temperature-dependent transformation strains, on SMA mechanics will be shown. It is worth pointing out that, within present explicit framework and addressing non-isothermal conditions, the value of $\sigma_{d/r}^{+/-}$ and $\varepsilon_{D/R}^{+/-}$ at the reference temperature $\overline{T}$ (at $\tau = \overline{t}$) can be considered in the governing equations at each incremental step. Accordingly, present model does not require to fix a specific form of interpolation functions for transformation lines in phase diagram (assumed piecewise-linear in most modeling approaches), as well as for the temperature-dependence of transformation strains, resulting in a very general and flexible tool for describing very different pseudo-elastic behaviors.

ACKNOWLEDGMENTS

The author gratefully acknowledges Prof. Franco Maceri, Prof. Giuseppe Vairo and Prof. Michel Frémond for fruitful discussions on this paper. This work was developed within the framework of Lagrange Laboratory, a European French-Italian research group. Present research study was supported by MIUR (PRIN, grant number F11J12000210001).

REFERENCES

[1] Shape Memory Alloys. Modeling and Engineering Applications, Lagoudas, D.C. (Ed.), Springer Science+BusinessMedia, LLC, New York, USA, (2008).

[2] Songa, G., Ma, N., Li, H.-N., Applications of shape memory alloys in civil structures. Engineering Structures, 28 (2006) 1266-1274.

[3] Auricchio, F., Marfia, S., Sacco, E., Modeling of SMA materials: training and two way shape memory effects, Computers and Structures, 81 (2003) 2301-2317.

[4] Auricchio, F., Bonetti, E., Scalet, G.,Ubertini, F., Theoretical and numerical modeling of shape memory alloys accounting for multiple phase transformations and martensite reorientation. International Journal of Plasticity, 59 (2014) 30-54.

[5] Moumni, Z., Zaki, W., Son, N.-Q., Theoretical and numerical modeling of solid-solid phase change: Application to the description of the thermomechanical behavior of shape memory alloys, International Journal of Plasticity, 24 (2008) 614-645.

[6] Churchill, C.B., Shaw, J.A., Iadicola, M.A., Tips and tricks for characterizing shape memory alloy wire: part 4 - Thermo-mechanical coupling, Experimental techniques, 34 (2010) 63-80.
[7] Khandelwal, A., Buravalla, V., Models for shape memory alloy behavior: an overview of modeling approaches. International Journal of Structural Changes in Solids, 1 (2009) 111-148.
[8] Coleman B.D., M.E. Gurtin, Thermodynamics with internal state variables. Department of Mathematical Sciences. Mellon College of Science, (1967) 1-72.
[9] Bouvet, C., Calloch, S., Lexcellent C., A phenomenological model for pseudoelasticity of shape memory alloys under multiaxial proportional and nonproportional loadings, European Journal of Mechanics A/Solids, 23 (2004) 37--61.
[10] Evangelista, V., Marfia, S., Sacco, E., A 3D sma constitutive model in the framework of finite strain. International Journal for Numerical Methods in Engineering, 81 (2010) 761-785.
[11] Leclercq, S., Lexcellent, C., A general macroscopic description of the thermomechanical behavior of shape memory alloys. Journal of the Mechanics and Physics of Solids, 44 (1996) 953-980.
[12] Nguyen, Q.S., Moumni, Z., Sur une modélisation du changement de phases solides, Comptes Rendus de l'Académie des Sciences. Series II, 321 (1995) 87-92.
[13] Halphen B., Nguyen, Q.S., Sur les matériaux standard généralisés, Journal de Mécanique, 14 (1975) 39-63.
[14] Lagoudas, D., Hartl, D., Chemisky, Y., Machado, L., Popov, P., Constitutive model for the numerical analysis of phase transformation in polycrystalline shape memory alloys, International Journal of Plasticity, 32-33 (2012) 155-183.
[15] Moreau, J.J., Sur les lois de frottement, de viscosité et de plasticité. Comptes Rendus de l'Académie des Sciences, 271 (1970) 608-611.
[16] Frémond, M., Phase Change in Mechanics. Lecture Notes of the Unione Matematica Italiana. Springer-Verlag, Berlin-Heidelberg, (2012).
[17] Frémond, M., Non-smooth thermomechanics. Springer-Verlag, Berlin, (2002).
[18] Baêta-Neves, A.P., Savi, M.A., Pacheco, P.M.C.L., On the Fremond's constitutive model for shape memory alloys. Mechanics Research Communication, 31 (2004) 677-688.
[19] Savi, M.A., Paiva, A., Baêta-Neves, A.P., Pacheco, P.M.C.L., Phenomenological modeling and numerical simulation of shape memory alloys: A thermo-plastic-phase transformation coupled model, Journal of Intelligent Material Systems and Structures, 13 (2002) 261-273.
[20] Pagano, S., Alart, P., Maisonneuve, O., Solid-solid phase transition modelling. Local and global minimizations of non-convex and relaxed potentials. Isothermal case for shape memory alloys, International Journal of Engineering Science, 36 (1998) 1143-1172.
[21] Zaki, W., Moumni, Z., A three-dimensional model of the thermomechanical behavior of shape memory alloys, Journal of the Mechanics and Physics of Solids, 55 (2007) 2455-2490.
[22] Ahlers, M., The martensitic transformation, Revista Matéria, 9 (2004) 169-183.